AGU ADVANCING EARTH AND SPACE SCIENCE

Geophysical Research Letters

RESEARCH LETTER
10.1029/2020GL091944

# The Synergistic Role of Sulfuric Acid, Bases, and Oxidized Organics Governing New-Particle Formation in Beijing

**Chao Yan[1,2], Rujing Yin[3], Yiqun Lu[4], Lubna Dada[2], Dongsen Yang[5], Yueyun Fu[3], Jenni Kontkanen[2], Chenjuan Deng[3], Olga Garmash[2], Jiaxin Ruan[5], Rima Baalbaki[2], Meredith Schervish[6], Runlong Cai[3], Matthew Bloss[2], Tommy Chan[2], Tianzeng Chen[7], Qi Chen[8], Xuemeng Chen[2], Yan Chen[9], Biwu Chu[2,7], Kaspar Dällenbach[2], Benjamin Foreback[2], Xucheng He[2], Liine Heikkinen[2], Tuija Jokinen[2], Heikki Junninen[2,10], Juha Kangasluoma[1,2], Tom Kokkonen[2], Mona Kurppa[2], Katrianne Lehtipalo[2,11], Haiyan Li[3], Hui Li[1], Xiaoxiao Li[3], Yiliang Liu[4], Qingxin Ma[7], Pauli Paasonen[2], Pekka Rantala[2], Rosaria E. Pileci[12], Anton Rusanen[2], Nina Sarnela[2], Pauli Simonen[13], Shixian Wang[1], Weigang Wang[9], Yonghong Wang[2], Mo Xue[3], Gan Yang[4], Lei Yao[2], Ying Zhou[1], Joni Kujansuu[1,2], Tuukka Petäjä[1,2,14], Wei Nie[14], Yan Ma[5], Maofa Ge[9], Hong He[7], Neil M. Donahue[6], Douglas R. Worsnop[14,15], Veli-Matti Kerminen[2], Lin Wang[4], Yongchun Liu[1], Jun Zheng[5], Markku Kulmala[1,2,14], Jingkun Jiang[3], and Federico Bianchi[1,2]**

[1]Beijing Advanced Innovation Center for Soft Matter Science and Engineering, Aerosol and Haze Laboratory, Beijing University of Chemical Technology, Beijing, China, [2]Institute for Atmospheric and Earth System Research/Physics, Faculty of Science, University of Helsinki, Helsinki, Finland, [3]School of Environment, State Key Joint Laboratory of Environment Simulation and Pollution Control, Tsinghua University, Beijing, China, [4]Department of Environmental Science & Engineering, Fudan University, Shanghai, China, [5]Jiangsu Key Laboratory of Atmospheric Environment Monitoring and Pollution Control, Nanjing University of Information Science & Technology, Nanjing, China, [6]Center for Atmospheric Particle Studies, Carnegie Mellon University, Pittsburgh, PA, USA, [7]Research Center for Eco-Environmental Sciences, Chinese Academy of Science, Beijing, China, [8]School of Environmental Sciences, Peking University, Beijing, China, [9]Institute of Chemistry, Chinese Academy of Sciences, Beijing, China, [10]Laboratory of Environmental Physics, Institute of Physics, University of Tartu, Tartu, Estonia, [11]Finnish Meteorological Institute, Helsinki, Finland, [12]Laboratory of Atmospheric Chemistry, Paul Scherrer Institute (PSI), Villigen, Switzerland, [13]Aerosol Physics Laboratory, Physics Unit, Tampere University, Tampere, Finland, [14]School of Atmospheric Sciences, Joint International Research Laboratory of Atmospheric and Earth System Sciences, Nanjing University, Nanjing, China, [15]Aerodyne Research Inc., Billerica, MA, USA

**Abstract** Intense and frequent new particle formation (NPF) events have been observed in polluted urban environments, yet the dominant mechanisms are still under debate. To understand the key species and governing processes of NPF in polluted urban environments, we conducted comprehensive measurements in downtown Beijing during January–March, 2018. We performed detailed analyses on sulfuric acid cluster composition and budget, as well as the chemical and physical properties of oxidized organic molecules (OOMs). Our results demonstrate that the fast clustering of sulfuric acid ($H_2SO_4$) and base molecules triggered the NPF events, and OOMs further helped grow the newly formed particles toward climate- and health-relevant sizes. This synergistic role of $H_2SO_4$, base species, and OOMs in NPF is likely representative of polluted urban environments where abundant $H_2SO_4$ and base species usually co-exist, and OOMs are with moderately low volatility when produced under high $NO_x$ concentrations.

**Plain Language Summary** Atmospheric new particle formation (NPF) is a dominant source of atmospheric ultrafine particles worldwide. Those particles profoundly influence climate and human health. NPF includes two consecutive processes, that is, the formation of new particles (~2 nm in diameter) and their subsequent growth to larger sizes. Extensive studies conducted in the laboratory and in forested areas have shown that many gaseous species can participate in NPF, such as sulfuric acid, ammonia, amines, and oxidize organic molecules. However, the actual roles of these vapors may vary significantly from location to location and are largely unclear in urban environments. Here, based on measurements of sulfuric acid, sulfuric acid clusters, and oxidize organic molecules, we demonstrate that sulfuric acid and base molecules were responsible for the initial formation of new particles during a wintertime field campaign in Beijing. The majority of oxidized organic molecules had a minor

**Key Points:**

- Process-level understanding of new particle formation (NPF) in wintertime Beijing was obtained based on measurement state-of-the-art instruments
- The analysis of sulfuric acid cluster composition and budget showed that sulfuric acid-base clustering initiated NPF
- Condensable organic vapors were characterized and demonstrated to have a crucial influence on the growth of newly formed particles

**Supporting Information:**

Supporting Information may be found in the online version of this article.

**Correspondence to:**

Y. Liu, J. Zheng, M. Kulmala, J. Jiang, and F. Bianchi,
liuyc@buct.edu.cn;
zheng.jun@nuist.edu.cn;
markku.kulmala@helsinki.fi;
jiangjk@tsinghua.edu.cn;
Federico.bianchi@helsinki.fi

**Citation:**

Yan, C., Yin, R., Lu, Y., Dada, L., Yang, D., Fu, Y., et al. (2021). The synergistic role of sulfuric acid, bases, and oxidized organics governing new-particle formation in Beijing. *Geophysical Research Letters*, *48*, e2020GL091944. https://doi.org/10.1029/2020GL091944

Received 4 DEC 2020
Accepted 7 MAR 2021

**Author Contributions:**

**Conceptualization:** Chao Yan, Yongchun Liu, Jun Zheng, Markku Kulmala, Jingkun Jiang, Federico Bianchi
**Formal analysis:** Chao Yan, Rujing Yin, Yiqun Lu, Lubna Dada, Dongsen Yang, Yueyun Fu
**Funding acquisition:** Weigang Wang, Yan Ma, Maofa Ge, Hong He, Neil M.

Donahue, Lin Wang, Yongchun Liu, Jun Zheng, Markku Kulmala, Jingkun Jiang
**Investigation:** Chao Yan, Rujing Yin, Lubna Dada, Dongsen Yang, Yueyun Fu, Jenni Kontkanen, Chenjuan Deng, Olga Garmash, Jiaxin Ruan, Rima Baalbaki, Meredith Schervish, Runlong Cai, Matthew Bloss, Tommy Chan, Tianzeng Chen, Xuemeng Chen, Yan Chen, Biwu Chu, Kaspar Dällenbach, Tom Kokkonen, Mona Kurppa, Katrianne Lehtipalo, Haiyan Li, Hui Li, Xiaoxiao Li, Yiliang Liu, Qingxin Ma, Pauli Paasonen, Pekka Rantala, Rosaria E. Pileci, Anton Rusanen, Nina Sarnela, Pauli Simonen, Shixian Wang, Weigang Wang, Yonghong Wang, Mo Xue, Gan Yang, Lei Yao, Ying Zhou, Wei Nie
**Project Administration:** Joni Kujansuu
**Supervision:** Tuukka Petäjä, Douglas R. Worsnop, Lin Wang, Yongchun Liu, Jun Zheng, Markku Kulmala, Jingkun Jiang, Federico Bianchi
**Writing – original draft:** Chao Yan
**Writing – review & editing:** Chao Yan, Lubna Dada, Douglas R. Worsnop, Veli-Matti Kerminen, Markku Kulmala, Jingkun Jiang, Federico Bianchi

contribution to the formation of new particles but were crucial for particle growth above 2–3 nm to climate- and health-relevant sizes.

## 1. Introduction

Atmospheric aerosol particles substantially affect climate and human health (Heal et al., 2012). Most aerosol particles in the Earth's atmosphere, including a large fraction of cloud condensation nuclei (CCN), are thought to originate from formation of atmospheric clusters and their subsequent growth to larger sizes (Gordon et al., 2017; Merikanto et al., 2009; Spracklen et al., 2008). This process is known as new particle formation (NPF). NPF occurs in almost all continental environments with varying frequencies and intensities (Chen et al., 2012; Kalafut-Pettibone et al., 2011; Kerminen et al., 2018; Kulmala et al., 2017; Mönkkönen et al., 2005; Nieminen et al., 2018; Peng et al., 2014; Qi et al., 2015; Wu et al., 2007; Xiao et al., 2015; Yao et al., 2018), and therefore, understanding the underlying mechanisms is an on-going research topic of high importance.

In spite of high primary aerosol emissions, NPF is a major source of ultrafine particles in polluted urban environments (Guo et al., 2014; Kulmala et al., 2016; Wang, Wu, Yue, et al., 2017). Studies have also suggested that NPF in urban environments contributes more to the CCN budget than it does in regional or remote environments (Peng et al., 2014; Wang, Wu, Yue, et al., 2017). In addition, NPF may also lead to haze under stagnant air conditions (Guo et al., 2014; Kulmala et al., 2021). Previous studies have suggested that high aerosol surface concentration is one primary parameter that governs the occurrence of NPF in polluted environments (Cai, Yang, et al., 2017; Deng et al., 2021; McMurry et al., 2005). Another recent study has predicted that little NPF should occur in polluted megacities due to the high condensation sink (CS) (Kulmala et al., 2017); by contrast, observations show that NPF in these areas are frequent and more intense than in clean environments (Deng et al., 2020). This discrepancy underlines an incomplete understanding of NPF in polluted and usually chemically complex environments.

Up to now, the driving mechanisms and key contributing species in both atmospheric clustering and subsequent growth in urban environments remain to be elucidated. For instance, a recent study has shown that clustering of gaseous sulfuric acid ($H_2SO_4$) and dimethylamine ($C_2H_7N$) is responsible for the initial steps of NPF in Shanghai (Yao et al., 2018). However, another recent laboratory-based study suggested that low-volatility organic vapors from the oxidation of vehicle-emitted organics, rather than $H_2SO_4$, can initiate the NPF in some urban environments (Guo et al., 2020). In addition, it was recently suggested that various dicarboxylic acids (diacids) could also cluster with $H_2SO_4$ and $C_2H_7N$ to initiate NPF (Fang et al., 2020).

Moreover, the contribution of low-volatility organic vapors to the NPF in the polluted urban atmosphere is largely unclear. These vapors form via the atmospheric oxidation of various volatile organic compounds (VOCs). It is widely acknowledged that low-volatility organic vapors are likely dominant contributors to the growth of freshly formed molecular clusters, allowing them to survive the scavenging in the atmosphere (e.g., Riipinen et al., 2011; Smith et al., 2008). Such contribution is controlled by both the concentration and saturation vapor pressures of low-volatility organic vapors (Donahue et al., 2013). Extensive studies that have been conducted in remote forested areas demonstrated that organic vapors, formed via the oxidation of monoterpenes, are able to contribute to the particle growth below 2 nm (Kulmala et al., 2013; Mohr et al., 2017). By contrast, the chemical characteristics of these low-volatility vapors in urban settings are under-studied, and the potential contribution of these vapors to NPF remains to be evaluated.

To advance our understanding of NPF in urban environments, we built a station in downtown Beijing equipped with state-of-the-art instruments. Our measurements cover most of atmospheric species directly contributing to NPF and particle evolution over a wide diameter range (1 nm–10 μm). Our comprehensive measurements allow for molecular-level analyses on NPF, upon which we determine the critical NPF processes and demonstrate the roles of different species in these processes.

## 2. Methodology

### 2.1. Measurement Station

The measurement was conducted at the Aerosol and Haze Laboratory/Beijing University of Chemical Technology station (AHL/BUCT station). The station is located in the main teaching building of the west cam-

pus of Beijing University of Chemical Technology (Lat. 39°56′31″ and Lon. 116°17′52″). The building is surrounded residential and commercial areas. In addition, there are three main roads within 600 m around the station. Therefore, the AHL/BUCT Station is a typical urban observation station affected by heavy traffic and residential emissions. More details about the station can be found elsewhere (Liu et al., 2020).

### 2.2. Instrumentation

The particle number concentration and size distribution over in the diameter range of 1 nm–10 μm were measured by a diethylene glycol scanning mobility particle spectrometer (DEG-SMPS, 1–7.5 nm) and a particle size distribution system (3 nm–10 μm). Additionally, the number concentration of clusters with a diameter range of 1.3–2.5 nm was measured with a Particle Sizer Magnifier, which showed good agreement with the DEG-SMPS measurements. The particle formation rate ($J_{1.5}$) was calculated for all NPF cases based on these data sets using the new-balance formula optimized for polluted environments (Cai & Jiang, 2017). $H_2SO_4$ and oxidized organic molecule (OOM) concentrations were measured with nitrate ion-based Chemical Ionization Atmospheric Pressure interface Time-of-Flight mass spectrometer (CI-APi-TOF, Aerodyne Research, Inc.). This instrument was calibrated for both the sensitivity to $H_2SO_4$ and the mass-dependent transmission efficiency. The molecular ion cluster composition was measured with an Atmospheric Pressure interface Time-of-Flight mass spectrometer (APi-TOF, Aerodyne Research, Inc.). The OOM volatility was estimated based on the parameterization by Mohr et al. (2019) and further corrected using the ambient temperature. More details of these instruments and other ancillary measurements are provided in the supporting information.

## 3. Results and Discussion

### 3.1. The Frequent Occurrence of NPF Events and the Governing Factors

We extend the mechanistic understanding of NPF in wintertime Beijing based on the results from intensive measurements conducted during January 23–March 31, 2018 at the newly built station in downtown Beijing. In Figure S1, we present the measurement overview, including the particle number concentration and size distribution over a wide size-range from 1 nm to 10 μm, relevant meteorological variables (temperature and UVB radiation intensity), calculated particle formation rate at 1.5 nm ($J_{1.5}$), CS, as well as gas-phase concentrations of vapors plausibly contributing to NPF (i.e., $H_2SO_4$ and OOMs). Details of these measurements and calculations are provided in the supporting information. We classify the whole measurement period into NPF and nonNPF days following the widely used method suggested in previous studies (Dal Maso et al., 2005). During the measurements, we observed NPF events frequently (32 out of 69 days), and during the first five weeks from 23 January to 28 February, NPF occurred on more than 60% of the days. The reduced NPF frequency in March is clearly associated with high CS, which is usually encountered when air masses come from polluted areas located on the south and east of Beijing. This is also consistent with an earlier study conducted at another site in Beijing (Cai, Yang, et al., 2017).

Comparisons of different variables between NPF and nonNPF days are shown in Figure 1. In the present-day continental boundary layer, it is widely accepted that $H_2SO_4$ and low-volatility organic species are crucial species for NPF (Lehtipalo et al., 2018; Riccobono et al., 2012, 2014; Rose et al., 2018; Yao et al., 2018). However, both $H_2SO_4$ monomer and total OOM concentrations in our observations were higher on nonNPF days than on NPF days (Figures 1b and 1d), likely due to the higher precursor concentrations ($SO_2$ and VOCs). Note that this observation should not be interpreted as indicating that $H_2SO_4$ and OOMs do not participate in NPF, but rather that enhanced clustering can be outcompeted by the simultaneously elevated loss of clusters to the condensation sink (i.e., higher CS, Figure 1e). The competition between $H_2SO_4$ clustering and CS is reflected in the $H_2SO_4$ dimer concentration, which is lower on nonNPF days due to the enhanced scavenging (Figure 1c). The close association between $H_2SO_4$ dimer and NPF occurrence and intensity will be discussed in detail in the next section. Furthermore, the temperature can influence NPF by modifying the formation and volatility of OOMs (Simon et al., 2020; Stolzenburg et al., 2018) and affecting the stability of $H_2SO_4$ clusters (Almeida et al., 2013). However, the mean temperature in NPF and nonNPF days was almost identical (Figure 1f), suggesting that temperature does not determine the NPF occurrence during our measurement period.

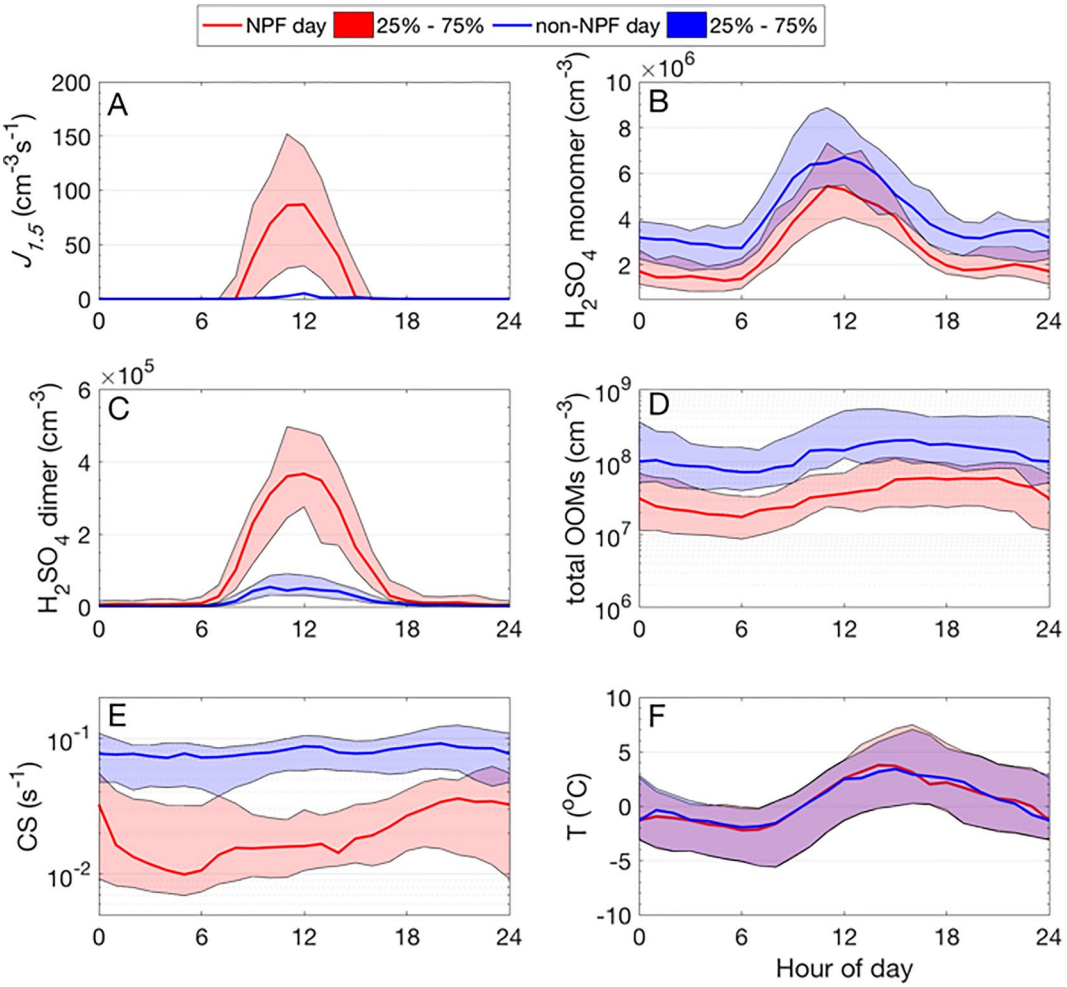


**Figure 1.** Diurnal variations of particle formation rates as well as relevant species and parameters in new particle formation (NPF) and nonNPF days. Lines are the median values, and shaded areas denote the 25%–75% of the data variation.

### 3.2. Intense New Particle Formation Driven by Acid-Base Clustering

In addition to the high frequency, NPF also occurred with high intensities, with a median $J_{1.5}$ of 86 $cm^{-3}$ $s^{-1}$ at peak hours (Figure 1a). The high particle formation rates appear to be a common characteristic of NPF in the polluted urban atmosphere, such as Shanghai (Xiao et al., 2015; Yao et al., 2018), Nanjing (Yu et al., 2016), and Barcelona (Brean et al., 2020). These particle formation rates are usually 1–2 orders of magnitude higher than those in relatively clean environments (Kulmala et al., 2013), suggesting the existence of abundant and efficient nucleation species in an urban atmosphere.

In Figure 2a, we show how the particle formation rate $J_{1.5}$ changes as a function of $H_2SO_4$ concentration. Despite an overall weak correlation between $J_{1.5}$ and $H_2SO_4$ monomer concentration, strong correlation becomes visible within narrow ranges of CS. This suggests that while $H_2SO_4$ drives the initial steps of NPF (i.e., the formation of embryonic clusters), CS plays a crucial role in determining the NPF intensity. For instance, at the same $H_2SO_4$ monomer concentration, $J_{1.5}$ may vary up to 3–4 orders of magnitude when CS ranges from 0.001 to 0.1 $s^{-1}$. Therefore, such $J_{1.5}$-$H_2SO_4$ relationship should be interpreted with caution when inferring the NPF mechanism, especially when comparing relatively more polluted ambient data with chamber results, because chambers usually have a lower CS (Dada et al., 2020). In our case, the $J_{1.5}$-$H_2SO_4$ relationship at CS < 0.02 $s^{-1}$ agrees well with the results of the CLOUD chamber experiments using

$H_2SO_4$ and dimethylamine ($C_2H_7N$) as the nucleating vapors (Kürten et al., 2018), suggesting that $H_2SO_4$ clustering that proceeds at similar efficiency is driving the initial steps of NPF.

To further confirm the high efficiency of $H_2SO_4$ cluster formation, we investigate the birth-death processes of $H_2SO_4$ dimers, that is, clusters containing two $H_2SO_4$ and also base molecules, which are the only $H_2SO_4$ clusters that can be reliably quantified. Other larger clusters also form, but they usually fall below the instrumental detection limit due to their low concentration and reduced ionization efficiency (thus low sensitivity) (Jen et al., 2016). As shown in Figure 2b, we found that the $H_2SO_4$ dimer concentration was in a pseudo steady-state between its formation rate by $H_2SO_4$ monomer collisions and its loss rate onto pre-existing larger particles by coagulation scavenging. The second-order rate constant between $H_2SO_4$ monomer collision forming one $H_2SO_4$ dimer is determined as $3.89 \times 10^{-10}$ $cm^3$ $s^{-1}$ (the fitted slope in Figure 2b), which is close to the theoretical molecular collision rate constant. Moreover, we observe a very strong correlation ($R^2 = 0.82$) between $J_{1.5}$ and $H_2SO_4$ dimer concentration (Figure 2c), showing that the abundance of $H_2SO_4$ clusters is directly associated with NPF intensity.

To further understand the high efficiency of $H_2SO_4$ clustering, we characterize the composition of $H_2SO_4$ cluster ions measured by the APi-TOF during the NPF events. As shown in Figure 2d, in addition to clusters consisting purely of $H_2SO_4$ (red dots in Figure 2d), amines ($C_2H_7N$, $C_3H_9N$, $C_4H_{11}N$) start to appear from the $H_2SO_4$ trimer onwards (magenta and blue dots in Figure 2d). The appearance of $C_2H_7N$ in the $H_2SO_4$ trimer is consistent with the results in the CLOUD chamber (Almeida et al., 2013). In addition, $C_3H_9N$ and $C_4H_{11}N$ participate in $H_2SO_4$ clustering at the same step; consistent with an earlier laboratory study with different amines (Jen et al., 2014), this suggests that $C_3H_9N$ and $C_4H_{11}N$ have a similar stabilizing effect on $H_2SO_4$ clusters. In fact, these amines form stable neutral clusters with one or two $H_2SO_4$. However, as suggested by our quantum chemical calculations using $C_2H_7N$ as a surrogate, deprotonation of these clusters will result in the loss of the amine moieties (see supporting information Section 3). Thus, large fractions of $HSO_4^-$ or $H_2SO_4HSO_4^-$ signals in our mass spectra come from $(H_2SO_4)_{1,2}$–$(C_{2-4}H_{7-11}N)_{1,2}$ clusters. Other base molecules, such as $CH_5N$ and $NH_3$ are involved in the cluster formation at later steps, as they are observed only in larger clusters. Moreover, unlike observations in forested areas and chamber experiments with the presence of both $H_2SO_4$ and biogenic VOCs (Lehtipalo et al., 2018; Riccobono et al., 2014; Schobesberger et al., 2013), $H_2SO_4$ clusters containing both base molecules and oxygenated organic molecules are not observed, suggesting little importance of multi-component nucleation. Altogether, we conclude that the initial steps of NPF, that is, the formation of 1.5 nm particles, is predominantly driven by acid-base clustering during the measurement period.

### 3.3. Characteristics of Oxygenated Organic Molecules and Their Role in NPF

In order to evaluate the role of low-volatility organic vapors in NPF, we measured organic molecules with the nitrate anion CI-APi-TOF (see more details in the supporting information). As we will demonstrate below, according to the latest definition of highly oxygenated organic molecules (HOMs) (Bianchi et al., 2019), most organic vapors that we detected in Beijing do not meet that requirement. Therefore, we use the term "oxygenated organic molecules (OOMs)" to refer to the measured compounds in this study. One should note that this instrument does not detect all OOMs, but it is specifically selective toward more oxidized ones, which are also most relevant for NPF (Ehn et al., 2014). In addition, we found this instrument to be sensitive to various nitrated phenols. However, these nitrated phenols are too volatile to have any noticeable contribution to NPF and are therefore excluded in this study. All identified OOMs together with their concentrations are listed in Table S2.

In Figure 3, we show chemical characteristics of OOMs based on the number of carbon atoms (nC), numbers of nitrogen atoms (nN), and effective oxygen atoms ($nO_{eff}$). The $nO_{eff}$ is calculated by disregarding the two oxygen atoms bonding with each nitrogen atom to reflect better the oxidation state and volatility of OOMs (Yan et al., 2020). These characteristics provide important information for understanding the critical processes in OOM formation.

Our first observation is that OOMs form through the oxidation of a complex mixture of VOCs. As suggested by the carbon distribution of OOMs that $C_{5-10}$ OOMs contribute to a dominant fraction of the total OOM concentration (Figure 3a), isoprene ($C_5$), alkylbenzenes ($C_{6-9}$), and monoterpenes ($C_{10}$) are

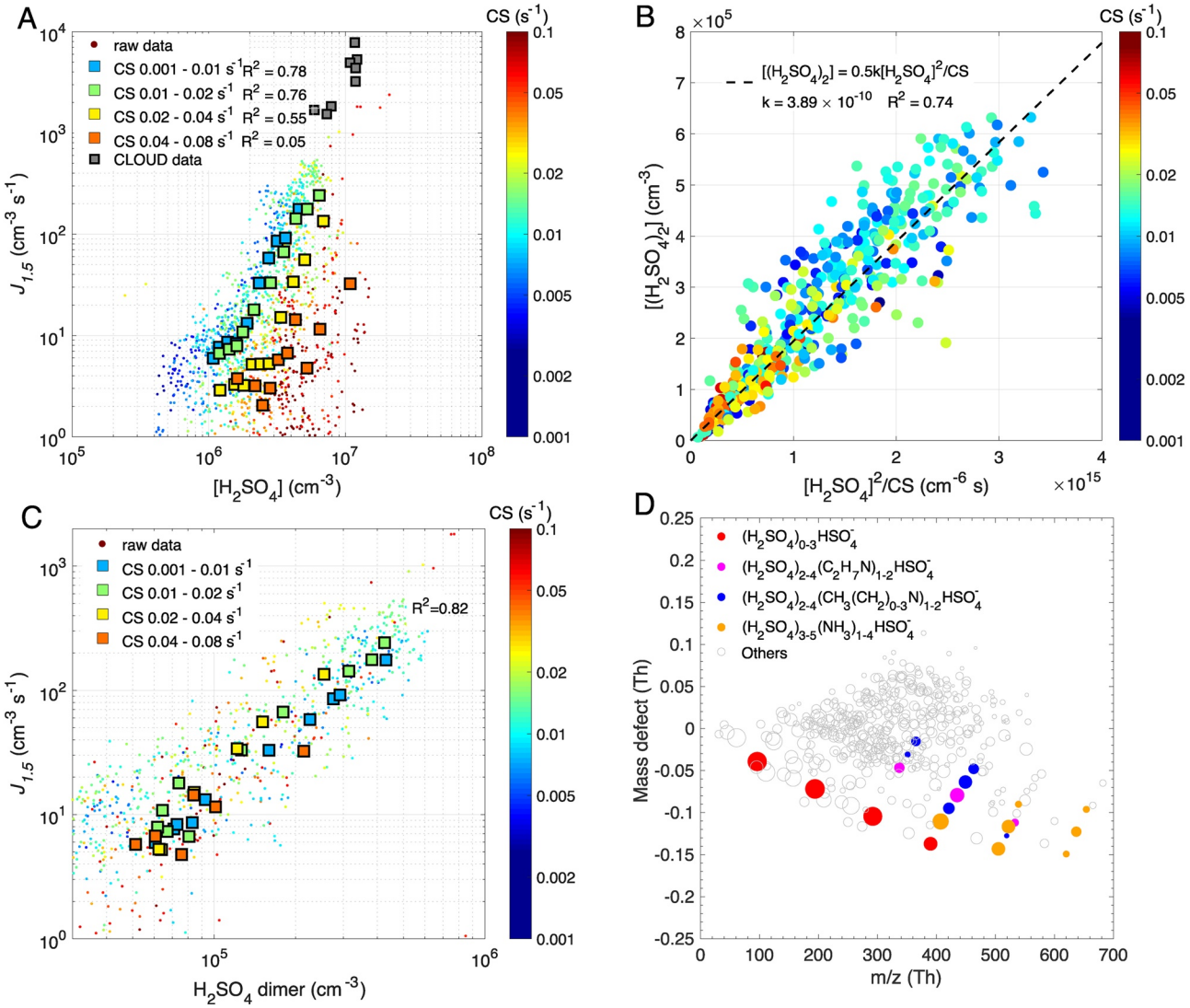


**Figure 2.** Illustration of the initial acid-base clustering in urban Beijing. (a) Particle formation rate $J_{1.5}$ as a function of $H_2SO_4$ monomer concentration ($[H_2SO_4]$). Both raw data (dots) and data binned to $H_2SO_4$ concentration at different condensation sink (CS) ranges (squares) are shown. Data from the CLOUD chamber experiments are shown in gray squares. The $R^2$ values are calculated with the raw data in each CS bin. (b) The relationship between sulfuric acid dimer concentration $[(H_2SO_4)_2]$, monomer concentration $[H_2SO_4]$, and the CS. The rate constant of sulfuric acid dimer formation is derived via the slope of a linear fit to the data. (c**)** Particle formation rate $J_{1.5}$ as a function of $[(H_2SO_4)_2]$. The data are binned in the same way as in (a). Both raw data (dots) and data binned data (squares) are shown. The $R^2$ is calculated with raw data. (d) A mass defect plot illustrating the chemical composition of natural ion clusters containing sulfuric acid and a variety of base molecules. Panels (a–c) are color-coded by CS. The size in (d) is logarithmically proportional to the signal intensity. It should be noted that, neutral $H_2SO_4$ and $H_2SO_4$ dimer concentrations were measured by the Chemical Ionization Atmospheric Pressure interface Time-of-Flight mass spectrometer (CI-APi-TOF) (a–c), while the $H_2SO_4$ cluster ion composition was obtained from the APi-TOF (d).

likely the most important precursor VOCs. In addition, $C_{3-4}$ OOMs might arise from the decomposition during the oxidation of VOCs with larger carbon numbers, and the $C_{>10}$ may come from the oxidation of polyaromatic hydrocarbons or from accretion reactions between two peroxy radicals ($RO_2$). However, it should be noted that, not all identified peaks in this study (Table S2) can be found in previous laboratory studies (Ehn et al., 2014; Krechmer et al., 2015; Molteni et al., 2018; Wang, Wu, Berndt et al., 2017, Wang et al., 2018). The difference in OOM composition may arise from the imperfect mimicking of the VOC oxidation under real atmospheric conditions in previous laboratory experiments, and also possibly results from some important but uncounted OOM sources, such as missing precursor VOCs and the evaporation from particulate phase.

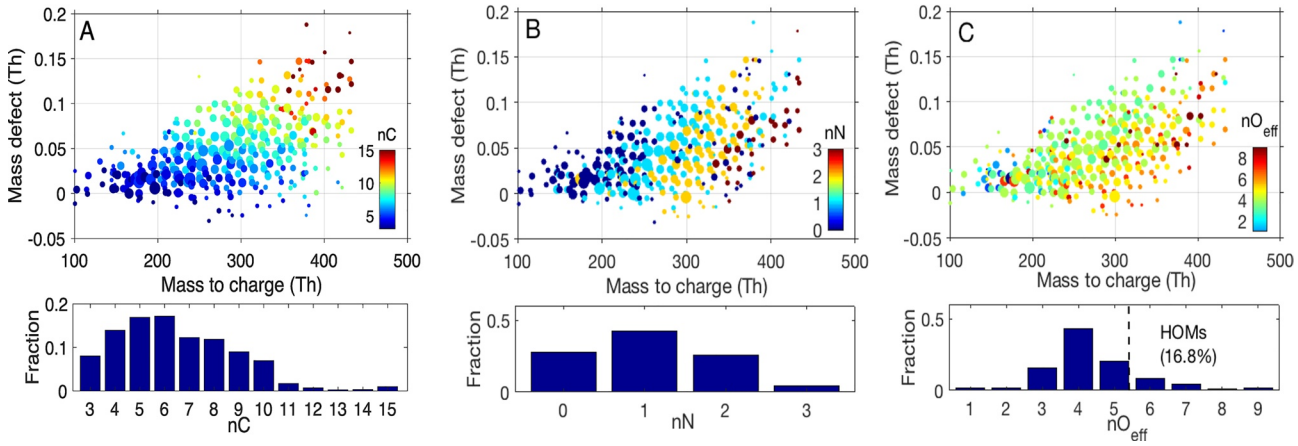


**Figure 3.** Chemical characteristics of oxidized organic molecules (OOMs) shown in mass defect plots. (a) Number of carbon (nC), (b**)** Number of nitrogen (nN). (c) Number of effective oxygen ($nO_{eff}$). Lower panels show the fractional distribution of the respective parameters.

Our second observation is that a major fraction (~75%) of OOMs are organic nitrates (Figure 3b), suggesting that the reaction of $RO_2 + NO_x$ is the main termination reaction pathway. In Beijing, the concentrations of peroxy radicals ($HO_2$ and $RO_2$) and $NO_x$ are in the ranges of $10^7$–$10^8$ $cm^{-3}$ and $10^{11}$–$10^{12}$ $cm^{-3}$, respectively (Tan et al., 2018). Given the fact that the reaction rate coefficient between $RO_2$ and $HO_2/RO_2$ is at most one order of magnitude higher than that between $RO_2$ and NO, the reactions of $RO_2 + RO_2$ or $RO_2 + HO_2$ are less important channels than the $RO_2 + NO_x$ channel in OOM formation. In addition to terminating the oxidation, the reaction of $RO_2 + NO$ can also propagate the oxidation by forming alkoxy radicals (RO), which does not lead to the formation of a nitrate group. As a result, it is likely that the actual contribution of the $RO_2 + NO_x$ reaction to the formation of OOMs is even greater than 75%. Furthermore, about 30% of OOMs contains two or three nitrogen atoms (Figure 3b). As indicated by the higher concentration during the day than at the night (Figure S2), the formation of such multiple nitrate groups was associated more with photochemistry than with the dark $NO_3$ chemistry. Multiple oxidation steps each followed by a $RO_2 + NO_x$ termination reaction could plausibly explain the formation of two or three nitrogen-containing compounds during daytime.

Our third observation is that HOMs in our measurements constituted a minor fraction of all OOMs. This could be explained by high NOx concentrations, which generally suppress $RO_2$ autoxidation (Figure 3c). From the literature, it is known that the degree of suppression is highly dependent on the precursor VOCs. For isoprene, 5 ppb NO is sufficient to completely shut down the autoxidation at 298 K (Wang et al., 2018). Due to the lower temperature during our measurement, which further slows down autoxidation, and higher $NO_x$ concentration, autoxidation in isoprene oxidation should be fully prevented. For monoterpenes, autoxidation should also be significantly suppressed. This is supported by the comparison of the $C_{10}H_{15}O_xN$ product distribution in Beijing and a boreal forest in southern Finland where the $NO_x$ concentration is much lower (Yan et al., 2016). As shown in Figure S3, relatively less oxygenated products ($C_{10}H_{15}O_{6\text{-}8}N$, $nO_{eff}$ = 4–6) are the main products, while highly oxygenated products ($C_{10}H_{15}O_{8\text{-}11}N$, $nO_{eff}$ = 6–9) at the boreal forest are dominant ones. For alkylbenzenes, the autoxidation rate of the bicyclic peroxy radicals (BPRs) varies by three orders of magnitude depending to the alkyl substitution group (Wang, Wu, Berndt, et al., 2017). The suggested maximum autoxidation rates of isopropyl-benzene, ethyl-benzene, toluene at 278 K are 9.2, 4.6, and 0.01 $s^{-1}$, respectively (Wang, Wu, Berndt, et al., 2017). These rates are equivalent to the bimolecular reaction rate with NO of about 38, 18, and 0.04 ppb, respectively, assuming a rate constant of $1 \times 10^{-11}$ $cm^3$ $s^{-1}$. Therefore, the autoxidation for alkylbenzenes with long-chain substituents (e.g., isopropyl-, ethyl-benzenes) should only be partially suppressed in Beijing, in contrast to the complete suppression of autoxidation for alkylbenzenes with short-chain substituents (e.g., methyl-, dimethyl-benzenes).

The volatility of OOMs is a key variable, linking the formation and chemical composition of OOMs to their potential contribution to the particle growth. We estimate the volatility distribution of the OOMs using a volatility basis set parameterization (see Section 2) (Bianchi et al., 2019; Chuang & Donahue, 2016). The overall

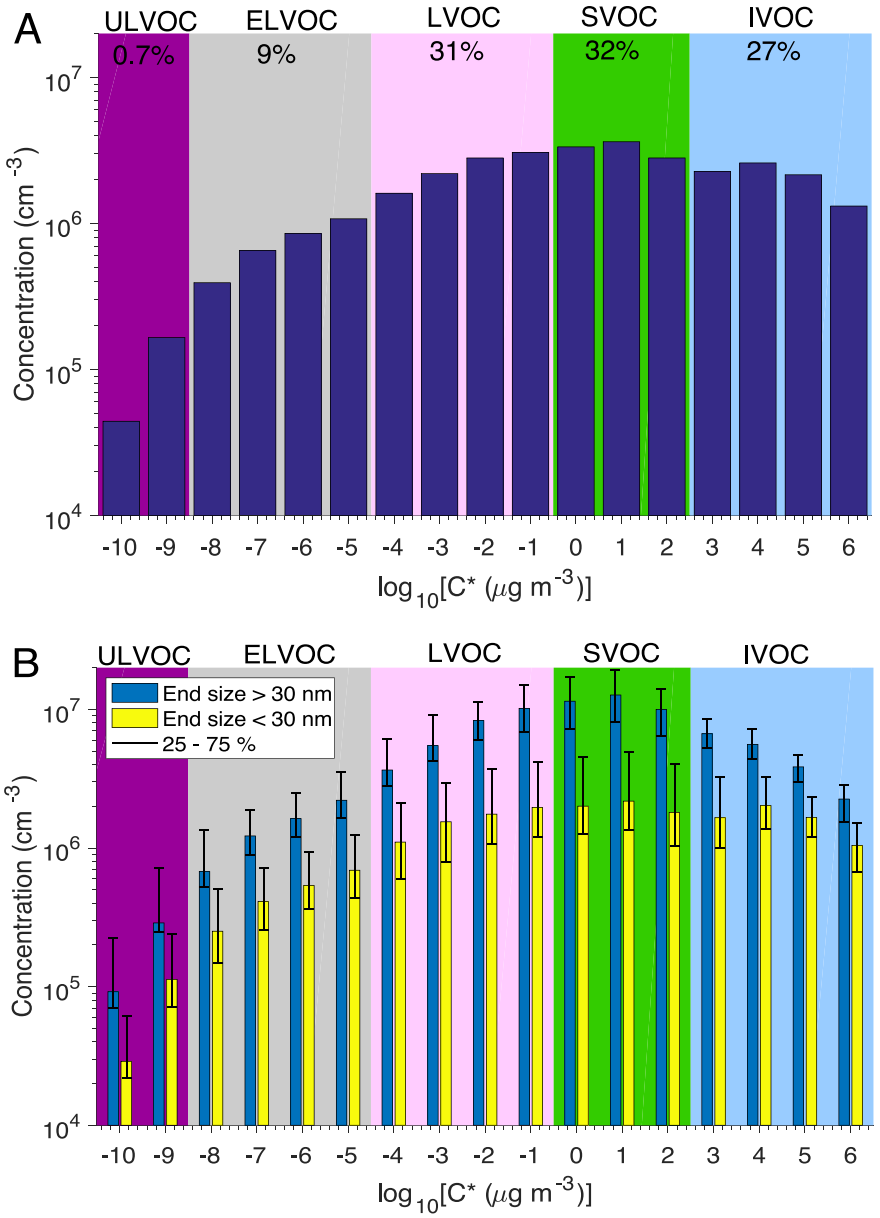


**Figure 4.** Volatility distribution of oxidized organic molecules observed with the nitrate Chemical Ionization Atmospheric Pressure interface Time-of-Flight mass spectrometer (CI-APi-TOF). The volatility is divided into different categories, including ultralow volatility organic compound (ULVOC), extremely low-volatility organic compound (ELVOC), low-volatility organic compound (LVOC), semi-volatile organic compound (SVOC), and intermediate volatile organic compound (IVOC). (a) the mean oxidized organic molecule (OOM) volatility distribution of OOMs during the new particle formation (NPF) periods of the campaign. Both mass saturation concentration (C*) and number saturation concentration (N*) are presented. (b) Mean volatility distributions in two different cases: The ending diameter is above 30 nm (blue) or below 30 nm (yellow). The end size is defined as the maximum diameter that the newly formed particles could reach within the event day.

binned volatility distribution is shown in Figure 4a. Based on our estimate, ultralow volatility organic compounds (ULVOC, $C^* \leq 3 \times 10^{-9}$ μg $m^{-3}$) that are capable of nucleating (Schervish & Donahue, 2020) are minor products, with a mean concentration of $2 \times 10^5$ $cm^{-3}$ (0.7% of total OOMs). This observation is also consistent with our former conclusion that the main NPF-relevant clustering process is $H_2SO_4$-base that does not involve OOMs. Also, only a small fraction of OOMs (9%, corresponding to an absolute concentration of $3 \times 10^6$ $cm^{-3}$) is extremely low-volatility organic compounds (ELVOC, $3 \times 10^{-9} < C^* \leq 1 \times 10^{-4.5}$ μg $m^{-3}$). Such low concen-

trations suggest that organic vapors are not the main driver of particle growth at the smallest size (e.g., ~2 nm). Consistent with this, an independent study based on $H_2SO_4$ measurement also indicates that $H_2SO_4$ and its clusters contribute significantly to the particle growth at 1.5–3 nm (Deng et al., 2020). ULVOCs are almost exclusively dimer compounds formed via association reactions between $RO_2$ radicals, while ELVOCs include both dimer compounds and highly oxygenated monomer compounds. Therefore, their low concentrations can be explained by the dominance of $RO_2$+$NO_x$ as the termination reaction, as we have discussed above.

Even though most OOMs (59%) in Beijing are semi-volatile organic compounds (SVOCs, $10^{-0.5} < C^* \leq 10^{2.5}$ μg $m^{-3}$) and intermediate volatile organic compounds (IVOC, $10^{2.5} < C^* \leq 10^{6.5}$ μg $m^{-3}$) that do not drive the growth of newly formed particles, a considerable fraction (31%) are low-volatility organic compounds (LVOCs, $10^{-4.5} < C^* \leq 10^{0.5}$ μg $m^{-3}$) that can contribute to the growth of particles above ~2 nm. This contribution is important for the survival of new particles against the scavenging loss. On NPF days, when newly formed particles grew beyond 30 nm, the concentration of OOMs was significantly higher than on days when particles did not reach 30 nm (Figure 4b). This suggests that condensable OOMs are crucial for particle growth from a few nanometers to a few tens of nanometers. It is worth noting that, the OOM volatility distribution in both cases were similar, indicating that the difference of OOMs was mainly caused by the overall VOC oxidation rate rather than a significant change in $RO_2$ + $NO_x$ chemistry, which can alter the OOM volatility distribution but not the overall concentration (Yan et al., 2020).

## 4. Conclusion

In summary, with state-of-the-art instruments, we track the particle evolution from molecules to clusters and then to particles. Based on such comprehensive measurements, we depict a complete picture of NPF in wintertime Beijing, including both the initial clustering and the subsequent cluster growth driven by different vapors. The clustering starts with the formation of thermodynamically stable sulfuric acid clusters at around 1–1.5 nm. This process in wintertime Beijing is driven by the acid-base clustering mechanism in the presence of abundant stabilizers, such as amines and $NH_3$. This is confirmed by our observations from many independent perspectives, including the J-$H_2SO_4$-CS relationship, the direct observation of molecular ion clusters by APi-TOF, and the low concentrations of ULVOC and ELVOC. This is in contrast to a recent suggestion made based on chamber experimental results that OOMs are solely responsible for NPF in Beijing. Nevertheless, OOMs are crucial for growing the newly formed particles through the very small sizes where they are vulnerable to scavenging loss. We confirm this, by quantifying each OOMs volatility classes. Overall, we clearly demonstrate that $H_2SO_4$, various bases species, and low-volatility organic vapors synergistically contributed to the intense NPF in wintertime Beijing, and in order to control the aerosol population, those key compounds need to be monitored and regulated.

## Conflict of Interest

The authors declare no conflict interest.

**Acknowledgment**
The work is supported by Academy of Finland via the Center of Excellence in Atmospheric Sciences (project no. 272041, 316114, 311932, and 315203) and European Research Council via ATM-GTP 266 (742206), CHAPAs (850614) and BLACARAT (615922), National Natural Science Foundation of China (41730106, 21876094, 91644213, and 92044301), and Samsung $PM_{2.5}$ SRP. NMD and MS are supported by the US NSF grant AGS-1801897. LW thanks the National Key R&D Program of China (2017YFC0209505 and 2017YFC0209503).

## Data Availability Statement

The measurement data used are available at ZENODO (https://zenodo.org, http://doi.org/10.5281/zenodo.4305410).

## References

Almeida, J., Schobesberger, S., Kürten, A., Ortega, I. K., Kupiainen-Määttä, O., Praplan, A. P., et al. (2013). Molecular understanding of sulphuric acid-amine particle nucleation in the atmosphere. *Nature*, *502*, 359–363. https://doi.org/10.1038/nature12663

Bianchi, F., Kurtén, T., Riva, M., Mohr, C., Rissanen, M. P., Roldin, P., et al. (2019). Highly oxygenated organic molecules (HOM) from gas-phase autoxidation involving peroxy radicals: A key contributor to atmospheric aerosol. *Chemical Reviews*, *119*, 3472–3509. https://doi.org/10.1021/acs.chemrev.8b00395

Brean, J., Beddows, D. C. S., Shi, Z., Temime-Roussel, B., Marchand, N., Querol, X., et al. (2020). Molecular insights into new particle formation in Barcelona, Spain. *Atmospheric Chemistry and Physics*, *20*, 10029–10045. https://doi.org/10.5194/acp-20-10029-2020

Cai, R., & Jiang, J. (2017). A new balance formula to estimate new particle formation rate: Reevaluating the effect of coagulation scavenging. *Atmospheric Chemistry and Physics*, *17*, 12659–12675. https://doi.org/10.5194/acp-17-12659-2017

Cai, R., Yang, D., Fu, Y., Wang, X., Li, X., Ma, Y., et al. (2017). Aerosol surface area concentration: A governing factor in new particle formation in Beijing. *Atmospheric Chemistry and Physics*, *17*, 12327–12340. https://doi.org/10.5194/acp-17-12327-2017

Chen, M., Titcombe, M., Jiang, J., Jen, C., Kuang, C., Fischer, M. L., et al. (2012). Acid-base chemical reaction model for nucleation rates in the polluted atmospheric boundary layer. *Proceedings of the National Academy of Sciences of the United States of America*, *109*, 18713–18718. https://doi.org/10.1073/pnas.1210285109

Chuang, W. K., & Donahue, N. M. (2016). A two-dimensional volatility basis set—Part 3: Prognostic modeling and NOx dependence. *Atmospheric Chemistry and Physics*, *16*, 123–134. https://doi.org/10.5194/acp-16-123-2016

Dada, L., Lehtipalo, K., Kontkanen, J., Nieminen, T., Baalbaki, R., Ahonen, L., et al. (2020). Formation and growth of sub-3-nm aerosol particles in experimental chambers. *Nature Protocols*, *15*, 1013–1040. https://doi.org/10.1038/s41596-019-0274-z

Dal Maso, M. D., Kulmala, M., Riipinen, I., & Wagner, R. (2005). Formation and growth of fresh atmospheric aerosols: Eight years of aerosol size distribution data from SMEAR II, Hyytiälä, Finland, *Boreal Environment Research*, *10*, 323–336.

Deng, C., Cai, R., Yan, C., Zheng, J., & Jiang, J. (2021). Formation and growth of sub-3 nm particles in megacities: Impact of background aerosols. *Faraday Discussions*, *226*, 348–363. https://doi.org/10.1039/d0fd00083c

Deng, C., Fu, Y., Dada, L., Yan, C., Cai, R., Yang, D., et al. (2020). Seasonal characteristics of new particle formation and growth in urban Beijing. *Environmental Science & Technology*, *54*, 8547–8557. https://doi.org/10.1021/acs.est.0c00808

Donahue, N. M., Ortega, I. K., Chuang, W., Riipinen, I., Riccobono, F., Schobesberger, S., et al. (2013). How do organic vapors contribute to new-particle formation? *Faraday Discussions*, *165*, 91–104. https://doi.org/10.1039/c3fd00046j

Ehn, M., Thornton, J. A., Kleist, E., Sipilä, M., Junninen, H., Pullinen, I., et al. (2014). A large source of low-volatility secondary organic aerosol. *Nature*, *506*, 476–479. https://doi.org/10.1038/nature13032

Fang, X., Hu, M., Shang, D., Tang, R., Shi, L., Olenius, T., et al. (2020). Observational evidence for the involvement of dicarboxylic acids in particle nucleation. *Environmental Science & Technology Letters*, *7*, 388–394. https://doi.org/10.1021/acs.estlett.0c00270

Gordon, H., Kirkby, J., Baltensperger, U., Bianchi, F., Breitenlechner, M., Curtius, J., et al. (2017). Causes and importance of new particle formation in the present-day and preindustrial atmospheres. *Journal of Geophysical Research: Atmospheres*, *122*, 8739–8760. https://doi.org/10.1002/2017jd026844

Guo, S., Hu, M., Peng, J., Wu, Z., Zamora, M. L., Shang, D., et al. (2020). Remarkable nucleation and growth of ultrafine particles from vehicular exhaust. *Proceedings of the National Academy of Sciences of the United States of America*, *117*, 3427–3432. https://doi.org/10.1073/pnas.1916366117

Guo, S., Hu, M., Zamora, M. L., Peng, J., Shang, D., Zheng, J., et al. (2014). Elucidating severe urban haze formation in China. *Proceedings of the National Academy of Sciences of the United States of America*, *111*, 17373–17378. https://doi.org/10.1073/pnas.1419604111

Heal, M. R., Kumar, P., & Harrison, R. M. (2012). Particles, air quality, policy and health. *Chemical Society Reviews*, *41*, 6606–6630. https://doi.org/10.1039/c2cs35076a

Jen, C. N., McMurry, P. H., & Hanson, D. R. (2014). Stabilization of sulfuric acid dimers by ammonia, methylamine, dimethylamine, and trimethylamine. *Journal of Geophysical Research: Atmospheres*, *119*, 7502–7514. https://doi.org/10.1002/2014jd021592

Jen, C. N., Zhao, J., McMurry, P. H., & Hanson, D. R. (2016). Chemical ionization of clusters formed from sulfuric acid and dimethylamine or diamines. *Atmospheric Chemistry and Physics*, *16*, 12513–12529. https://doi.org/10.5194/acp-16-12513-2016

Kürten, A., Li, C., Bianchi, F., Curtius, J., Dias, A., Donahue, N. M., et al. (2018). New particle formation in the sulfuric acid-dimethylamine-water system: Reevaluation of CLOUD chamber measurements and comparison to an aerosol nucleation and growth model. *Atmospheric Chemistry and Physics*, *18*, 845–863. https://doi.org/10.5194/acp-18-845-2018

Kalafut-Pettibone, A. J., Wang, J., Eichinger, W. E., Clarke, A., Vay, S. A., Blake, D. R., & Stanier, C. O. (2011). Size-resolved aerosol emission factors and new particle formation/growth activity occurring in Mexico City during the MILAGRO 2006 Campaign. *Atmospheric Chemistry and Physics*, *11*, 8861–8881. https://doi.org/10.5194/acp-11-8861-2011

Kerminen, V.-M., Chen, X., Vakkari, V., Petäjä, T., Kulmala, M., & Bianchi, F. (2018). Atmospheric new particle formation and growth: Review of field observations. *Environmental Research Letters*, *13*, 103003. https://doi.org/10.1088/1748-9326/aadf3c

Krechmer, J. E., Coggon, M. M., Massoli, P., Nguyen, T. B., Crounse, J. D., Hu, W., et al. (2015). Formation of low volatility organic compounds and secondary organic aerosol from isoprene hydroxyhydroperoxide low-NO oxidation. *Environmental Science & Technology*, *49*, 10330–10339. https://doi.org/10.1021/acs.est.5b02031

Kulmala, M., Dada, L., Daellenbach, K. R., Yan, C., Stolzenburg, D., Kontkanen, J., et al. (2021). Is reducing new particle formation a plausible solution to mitigate particulate air pollution in Beijing and other Chinese megacities? *Faraday Discussions*, *226*, 334–347. https://doi.org/10.1039/D0FD00078G

Kulmala, M., Kerminen, V.-M., Petäjä, T., Ding, A. J., & Wang, L. (2017). Atmospheric gas-to-particle conversion: Why NPF events are observed in megacities? *Faraday Discussions*, *200*, 271–288. https://doi.org/10.1039/c6fd00257a

Kulmala, M., Kontkanen, J., Junninen, H., Lehtipalo, K., Manninen, H. E., Nieminen, T., et al. (2013). Direct observations of atmospheric aerosol nucleation. *Science*, *339*, 943–946. https://doi.org/10.1126/science.1227385

Kulmala, M., Petäjä, T., Kerminen, V.-M., Kujansuu, J., Ruuskanen, T., Ding, A., et al. (2016). On secondary new particle formation in China. *Frontiers of Environmental Science & Engineering*, *10*. https://doi.org/10.1007/s11783-016-0850-1

Lehtipalo, K., Yan, C., Dada, L., Bianchi, F., Xiao, M., Wagner, R., et al. (2018). Multicomponent new particle formation from sulfuric acid, ammonia, and biogenic vapors. *Science Advances*, *4*, eaau5363. https://doi.org/10.1126/sciadv.aau5363

Liu, Y., Yan, C., Feng, Z., Zheng, F., Fan, X., Zhang, Y., et al. (2020). Continuous and comprehensive atmospheric observations in Beijing: A station to understand the complex urban atmospheric environment. *Big Earth Data*, *4*, 295–321. https://doi.org/10.1080/20964471.2020.1798707

McMurry, P. H., Fink, M., Sakurai, H., Stolzenburg, M. R., Mauldin, R. L., Smith, J., et al. (2005). A criterion for new particle formation in the sulfur-rich Atlanta atmosphere. *Journal of Geophysical Research*, *110*, 2935–2948. https://doi.org/10.1029/2005jd005901

Merikanto, J., Spracklen, D. V., Mann, G. W., Pickering, S. J., & Carslaw, K. S. (2009). Impact of nucleation on global CCN. *Atmospheric Chemistry and Physics*, *9*, 8601–8616. https://doi.org/10.5194/acp-9-8601-2009

Mohr, C., Lopez-Hilfiker, F. D., Yli-Juuti, T., Heitto, A., Lutz, A., Hallquist, M., et al. (2017). Ambient observations of dimers from terpene oxidation in the gas phase: Implications for new particle formation and growth. *Geophysical Research Letters*, *44*, 2958–2966. https://doi.org/10.1002/2017gl072718

Mohr, C., Thornton, J. A., Heitto, A., Lopez-Hilfiker, F. D., Lutz, A., Riipinen, I., et al. (2019). Molecular identification of organic vapors driving atmospheric nanoparticle growth. *Nature Communications*, *10*, 4442. https://doi.org/10.1038/s41467-019-12473-2

Molteni, U., Bianchi, F., Klein, F., El Haddad, I., Frege, C., Rossi, M. J., et al. (2018). Formation of highly oxygenated organic molecules from aromatic compounds. *Atmospheric Chemistry and Physics*, *18*, 1909–1921. https://doi.org/10.5194/acp-18-1909-2018

Mönkkönen, P., Koponen, I. K., Lehtinen, K. E. J., Hämeri, K., Uma, R., & Kulmala, M. (2005). Measurements in a highly polluted Asian mega city: Observations of aerosol number size distribution, modal parameters and nucleation events. *Atmospheric Chemistry and Physics*, *5*, 57–66. https://doi.org/10.5194/acp-5-57-2005

Nieminen, T., Kerminen, V.-M., Petäjä, T., Aalto, P. P., Arshinov, M., Asmi, E., et al. (2018). Global analysis of continental boundary layer new particle formation based on long-term measurements. *Atmospheric Chemistry and Physics*, *18*, 14737–14756. https://doi.org/10.5194/acp-18-14737-201

Peng, J. F., Hu, M., Wang, Z. B., Huang, X. F., Kumar, P., Wu, Z. J., et al. (2014). Submicron aerosols at thirteen diversified sites in China: Size distribution, new particle formation and corresponding contribution to cloud condensation nuclei production. *Atmospheric Chemistry and Physics*, *14*, 10249–10265. https://doi.org/10.5194/acp-14-10249-2014

Qi, X. M., Ding, A. J., Nie, W., Petäjä, T., Kerminen, V.-M., Herrmann, E., et al. (2015). Aerosol size distribution and new particle formation in the western Yangtze River Delta of China: 2 years of measurements at the SORPES station. *Atmospheric Chemistry and Physics*, *15*, 12445–12464. https://doi.org/10.5194/acp-15-12445-2015

Riccobono, F., Rondo, L., Sipilä, M., Barmet, P., Curtius, J., Dommen, J., et al. (2012). Contribution of sulfuric acid and oxidized organic compounds to particle formation and growth. *Atmospheric Chemistry and Physics*, *12*, 9427–9439. https://doi.org/10.5194/acp-12-9427-2012

Riccobono, F., Schobesberger, S., Scott, C. E., Dommen, J., Ortega, I. K., Rondo, L., et al. (2014). Oxidation products of biogenic emissions contribute to nucleation of atmospheric particles. *Science*, *344*, 717–721. https://doi.org/10.1126/science.1243527

Riipinen, I., Pierce, J. R., Yli-Juuti, T., Nieminen, T., Häkkinen, S., Ehn, M., et al. (2011). Organic condensation: A vital link connecting aerosol formation to cloud condensation nuclei (CCN) concentrations. *Atmospheric Chemistry and Physics*, *11*, 3865–3878. https://doi.org/10.5194/acp-11-3865-2011

Rose, C., Zha, Q., Dada, L., Yan, C., Lehtipalo, K., Junninen, H., et al. (2018). Observations of biogenic ion-induced cluster formation in the atmosphere. *Science Advances*, *4*, eaar5218. https://doi.org/10.1126/sciadv.aar5218

Schervish, M., & Donahue, N. M. (2020). Peroxy radical chemistry and the volatility basis set. *Atmospheric Chemistry and Physics*, *20*, 1183–1199. https://doi.org/10.5194/acp-20-1183-2020

Schobesberger, S., Junninen, H., Bianchi, F., Lonn, G., Ehn, M., Lehtipalo, K., et al. (2013). Molecular understanding of atmospheric particle formation from sulfuric acid and large oxidized organic molecules. *Proceedings of the National Academy of Sciences of the United States of America*, *110*, 17223–17228. https://doi.org/10.1073/pnas.1306973110

Simon, M., Dada, L., Heinritzi, M., Scholz, W., Stolzenburg, D., Fischer, L., et al. (2020). Molecular understanding of new-particle formation from α-pinene between −50 and +25°C. *Atmospheric Chemistry and Physics*, *20*, 9183–9207. https://doi.org/10.5194/acp-20-9183-2020

Smith, J. N., Dunn, M. J., VanReken, T. M., Iida, K., Stolzenburg, M. R., McMurry, P. H., & Huey, L. G. (2008). Chemical composition of atmospheric nanoparticles formed from nucleation in Tecamac, Mexico: Evidence for an important role for organic species in nanoparticle growth. *Geophysical Research Letters*, *35*, L04808. https://doi.org/10.1029/2007gl032523

Spracklen, D. V., Carslaw, K. S., Kulmala, M., Kerminen, V.-M., Sihto, S.-L., Riipinen, I., et al. (2008). Contribution of particle formation to global cloud condensation nuclei concentrations. *Geophysical Research Letters*, *35*, L06808. https://doi.org/10.1029/2007gl033038

Stolzenburg, D., Fischer, L., Vogel, A. L., Heinritzi, M., Schervish, M., Simon, M., et al. (2018). Rapid growth of organic aerosol nanoparticles over a wide tropospheric temperature range. *Proceedings of the National Academy of Sciences of the United States of America*, *115*, 9122–9127. https://doi.org/10.1073/pnas.1807604115

Tan, Z., Rohrer, F., Lu, K., Ma, X., Bohn, B., Broch, S., et al. (2018). Wintertime photochemistry in Beijing: Observations of ROx radical concentrations in the North China Plain during the BEST-ONE campaign. *Atmospheric Chemistry and Physics*, *18*, 12391–12411. https://doi.org/10.5194/acp-18-12391-2018

Wang, S., Riva, M., Yan, C., Ehn, M., & Wang, L. (2018). Primary formation of highly oxidized multifunctional products in the OH-initiated oxidation of isoprene: A combined theoretical and experimental study. *Environmental Science & Technology*, *52*, 12255–12264. https://doi.org/10.1021/acs.est.8b02783

Wang, S., Wu, R., Berndt, T., Ehn, M., & Wang, L. (2017). Formation of highly oxidized radicals and multifunctional products from the atmospheric oxidation of alkylbenzenes. *Environmental Science & Technology*, *51*, 8442–8449. https://doi.org/10.1021/acs.est.7b02374

Wang, Z., Wu, Z., Yue, D., Shang, D., Guo, S., Sun, J., et al. (2017). New particle formation in China: Current knowledge and further directions. *The Science of the Total Environment*, *577*, 258–266. https://doi.org/10.1016/j.scitotenv.2016.10.177

Wu, Z., Hu, M., Liu, S., Wehner, B., Bauer, S., Ma ßling, A., et al. (2007). New particle formation in Beijing, China: Statistical analysis of a 1-year data set. *Journal of Geophysical Research*, *112*, D09209. https://doi.org/10.1029/2006jd007406

Xiao, S., Wang, M. Y., Yao, L., Kulmala, M., Zhou, B., Yang, X., et al. (2015). Strong atmospheric new particle formation in winter in urban Shanghai, China. *Atmospheric Chemistry and Physics*, *15*, 1769–1781. https://doi.org/10.5194/acp-15-1769-2015

Yan, C., Nie, W., Äijälä, M., Rissanen, M. P., Canagaratna, M. R., Massoli, P., et al. (2016). Source characterization of highly oxidized multifunctional compounds in a boreal forest environment using positive matrix factorization. *Atmospheric Chemistry and Physics*, *16*, 12715–12731. https://doi.org/10.5194/acp-16-12715-2016

Yan, C., Nie, W., Vogel, A. L., Dada, L., Lehtipalo, K., Stolzenburg, D., et al. (2020). Size-dependent influence of NOx on the growth rates of organic aerosol particles. *Science Advances*, *6*, eaay4945. https://doi.org/10.1126/sciadv.aay4945

Yao, L., Garmash, O., Bianchi, F., Zheng, J., Yan, C., Kontkanen, J., et al. (2018). Atmospheric new particle formation from sulfuric acid and amines in a Chinese megacity. *Science*, *361*, 278–281. https://doi.org/10.1126/science.aao4839

Yu, H., Zhou, L., Dai, L., Shen, W., Dai, W., Zheng, J., et al. (2016). Nucleation and growth of sub-3 nm particles in the polluted urban atmosphere of a megacity in China. *Atmospheric Chemistry and Physics*, *16*, 2641–2657. https://doi.org/10.5194/acp-16-2641-2016

## References From the Supporting Information

Almeida, J., Schobesberger, S., Kürten, A., Ortega, I. K., Kupiainen-Määttä, O., Praplan, A. P., et al. (2013). Molecular understanding of sulphuric acid-amine particle nucleation in the atmosphere. *Nature*, *502*, 359–363. https://doi.org/10.1038/nature12663

Becke, A. D. (1988). Density-functional exchange-energy approximation with correct asymptotic behavior. *Physical Review A*, *38*, 3098. https://doi.org/10.1103/physreva.38.3098

Breitenlechner, M., Fischer, L., Hainer, M., Heinritzi, M., Curtius, J., & Hansel, A. (2017). PTR3: An instrument for studying the lifecycle of reactive organic carbon in the atmosphere. *Analytical Chemistry*, *89*, 5824–5831. https://doi.org/10.1021/acs.analchem.6b05110

Cai, R., Chandra, I., Yang, D., Yao, L., Fu, Y., Li, X., et al. (2018). Estimating the influence of transport on aerosol size distributions during new particle formation events. *Atmospheric Chemistry and Physics*, *18*, 16587–16599. https://doi.org/10.5194/acp-18-16587-2018

Cai, R., Chen, D.-R., Hao, J., & Jiang, J. (2017). A miniature cylindrical differential mobility analyzer for sub-3 nm particle sizing. *Journal of Aerosol Science*, *106*, 111–119. https://doi.org/10.1016/j.jaerosci.2017.01.004

Cai, R., & Jiang, J. (2017). A new balance formula to estimate new particle formation rate: Reevaluating the effect of coagulation scavenging. *Atmospheric Chemistry and Physics*, *17*, 12659–12675. https://doi.org/10.5194/acp-17-12659-2017

Cai, R., Yang, D., Fu, Y., Wang, X., Li, X., Ma, Y., et al. (2017). Aerosol surface area concentration: A governing factor in new particle formation in Beijing. *Atmospheric Chemistry and Physics*, *17*, 12327–12340. https://doi.org/10.5194/acp-17-12327-2017

Donahue, N. M., Epstein, S. A., Pandis, S. N., & Robinson, A. L. (2011). A two-dimensional volatility basis set: 1. Organic-aerosol mixing thermodynamics. *Atmospheric Chemistry and Physics*, *11*, 3303–3318. https://doi.org/10.5194/acp-11-3303-2011

Dunne, E. M., Gordon, H., Kurten, A., Almeida, J., Duplissy, J., Williamson, C., et al. (2016). Global atmospheric particle formation from CERN CLOUD measurements. *Science*, *354*, 1119–1124. https://doi.org/10.1126/science.aaf2649

Epstein, S. A., Riipinen, I., & Donahue, N. M. (2009). A semiempirical correlation between enthalpy of vaporization and saturation concentration for organic aerosol. *Environmental Science & Technology*, *44*, 743–748.

Grimme, S., Antony, J., Ehrlich, S., & Krieg, H. (2010). A consistent and accurate ab initio parametrization of density functional dispersion correction (DFT-D) for the 94 elements H-Pu. *The Journal of Chemical Physics*, *132*, 154104. https://doi.org/10.1063/1.3382344

Hättig, C., Klopper, W., Köhn, A., & Tew, D. P. (2012). Explicitly correlated electrons in molecules. *Chemical Reviews*, *112*, 4–74. https://doi.org/10.1021/cr200168z

Hyttinen, N., Kupiainen-Määttä, O., Rissanen, M. P., Muuronen, M., Ehn, M., & Kurtén, T. (2015). Modeling the charging of highly oxidized cyclohexene ozonolysis products using nitrate-based chemical ionization. *The Journal of Physical Chemistry A*, *119*, 6339–6345. https://doi.org/10.1021/acs.jpca.5b01818

Jiang, J., Chen, M., Kuang, C., Attoui, M., & McMurry, P. H. (2011). Electrical mobility spectrometer using a diethylene glycol condensation particle counter for measurement of aerosol size distributions down to 1 nm. *Aerosol Science and Technology*, *45*, 510–521. https://doi.org/10.1080/02786826.2010.547538

Jokinen, T., Sipilä, M., Junninen, H., Ehn, M., Lönn, G., Hakala, J., et al. (2012). Atmospheric sulphuric acid and neutral cluster measurements using CI-APi-TOF. *Atmospheric Chemistry and Physics*, *12*, 4117–4125. https://doi.org/10.5194/acp-12-4117-2012

Kangasluoma, J., Franchin, A., Duplissy, J., Ahonen, L., Korhonen, F., Attoui, M., et al. (2016). Operation of the Airmodus A11 nano condensation nucleus counter at various inlet pressures and various operation temperatures, and design of a new inlet system. *Atmospheric Measurement Techniques*, *9*, 2977–2988. https://doi.org/10.5194/amt-9-2977-2016

Kulmala, M., Petäjä, T., Nieminen, T., Sipilä, M., Manninen, H. E., Lehtipalo, K., et al. (2012). Measurement of the nucleation of atmospheric aerosol particles. *Nature Protocols*, *7*, 1651. https://doi.org/10.1038/nprot.2012.091

Kürten, A., Rondo, L., Ehrhart, S., & Curtius, J. (2012). Calibration of a chemical ionization mass spectrometer for the measurement of gaseous sulfuric acid. *The Journal of Physical Chemistry A*, *116*, 6375–6386. https://doi.org/10.1021/jp212123n

Lee, C., Yang, W., & Parr, R. G. (1988). Development of the Colle-Salvetti correlation-energy formula into a functional of the electron density. *Physical Review B: Condensed Matter*, *37*, 785–789. https://doi.org/10.1103/physrevb.37.785

Lippert, B. G., Parrinello, J. H. a. M., & Michele. (2010). A hybrid Gaussian and plane wave density functional scheme. *Molecular Physics*, *92*, 477–488. https://doi.org/10.1080/002689797170220

Liu, J., Jiang, J., Zhang, Q., Deng, J., & Hao, J. (2016). A spectrometer for measuring particle size distributions in the range of 3 nm to 10 μm. *Frontiers of Environmental Science & Engineering*, *10*, 63–72. https://doi.org/10.1007/s11783-014-0754-x

Mirme, S., & Mirme, A. (2013). The mathematical principles and design of the NAIS—A spectrometer for the measurement of cluster ion and nanometer aerosol size distributions. *Atmospheric Measurement Technique*, *6*, 1061–1071. https://doi.org/10.5194/amt-6-1061-2013

VandeVondele, J., Mohamed, F., Krack, M., Hutter, J., Sprik, M., & Parrinello, M. (2005). The influence of temperature and density functional models in ab initio molecular dynamics simulation of liquid water. *The Journal of Chemical Physics*, *122*, 014515. https://doi.org/10.1063/1.1828433

Vanhanen, J., Mikkilä, J., Lehtipalo, K., Sipilä, M., Manninen, H. E., Siivola, E., et al. (2011). Particle size magnifier for nano-CN detection. *Aerosol Science and Technology*, *45*, 533–542. https://doi.org/10.1080/02786826.2010.547889

Yan, C., Nie, W., Äijälä, M., Rissanen, M. P., Canagaratna, M. R., Massoli, P., et al. (2016). Source characterization of highly oxidized multifunctional compounds in a boreal forest environment using positive matrix factorization. *Atmospheric Chemistry and Physics*, *16*, 12715–12731. https://doi.org/10.5194/acp-16-12715-2016

Zhao, Y., & Truhlar, D. G. (2008). The M06 suite of density functionals for main group thermochemistry, thermochemical kinetics, noncovalent interactions, excited states, and transition elements: Two new functionals and systematic testing of four M06-class functionals and 12 other functionals. *Theoretical Chemistry Accounts*, *120*, 215–241. https://doi.org/10.1007/s00214-007-0310-x